



Original contribution

Assessing liver fibrosis in chronic hepatitis B using MR extracellular volume measurements: Comparison with serum fibrosis indices

He-qing Wang^{a,1}, Kai-pu Jin^{a,1}, Meng-su Zeng^a, Cai-zhong Chen^a, Sheng-xiang Rao^a, Yuan Ji^b, Cai-xia Fu^c, Ruo-fan Sheng^{a,*}

^a Department of Radiology, Zhongshan Hospital, Fudan University, Shanghai Institute of Medical Imaging, No. 180 Fenglin Road, Xuhui District, Shanghai 20032, China

^b Department of Pathology, Zhongshan Hospital, Fudan University, No. 180 Fenglin Road, Xuhui District, Shanghai 20032, China

^c Siemens Healthcare, Shanghai, China

ARTICLE INFO

Keywords:

Hepatic fibrosis
Extracellular space
Magnetic resonance imaging
Gadolinium

ABSTRACT

Objectives: To evaluate the diagnostic value of liver extracellular volume (ECV_{liver}) measurement by equilibrium MR in staging liver fibrosis in chronic hepatitis B (CHB) patients, and to compare its performance with serum fibrosis indices.

Materials and methods: 91 CHB patients were included and underwent gadopentetate dimeglumine-enhanced MRI with T1 mapping sequence before and 15-min after contrast. ECV_{liver}, aspartate aminotransferase-to-platelet ratio index (APRI) and fibrosis index based on the four factors (FIB-4) were calculated and compared between fibrosis subgroups, and the correlations between the three indices and fibrosis stage or inflammatory activity were measured by Spearman correlation analysis and stepwise multiple regression analysis. Diagnostic performance in evaluating liver fibrosis stage was assessed and compared using receiver operating characteristic analysis.

Results: Interobserver agreement showed an excellent interclass correlation coefficient of 0.895 for ECV_{liver}. ECV_{liver}, APRI and FIB-4 were different between fibrosis stages as a whole ($F/H = 18.44\text{--}24.36$, $P \leq 0.001$). ECV_{liver} had the strongest correlation with fibrosis stage ($r = 0.727$, $P < 0.001$), while APRI and FIB-4 had weak correlations ($r = 0.466$ and 0.440 , $P < 0.001$). Multivariate analysis showed that only ECV_{liver} was independently correlated with fibrosis stage ($P < 0.001$). The fibrosis stage was the only independent factor correlated with ECV_{liver} comparing to inflammatory activity ($P < 0.001$). AUCs of ECV_{liver} were larger than both APRI and FIB-4 in fibrosis staging, with significant differences in the diagnosis of advanced fibrosis ($\geq F3$) and cirrhosis (F4) ($P = 0.0024$ to 0.0049).

Conclusion: MR ECV_{liver} provides a promising noninvasive tool in staging liver fibrosis for CHB patients, superior to the fibrosis indices of APRI and FIB-4.

1. Introduction

Chronic hepatitis B (CHB) virus infection remains a significant global health problem which infected approximately 240 million individuals worldwide, and has a particularly high prevalence in Asia including China [1]. CHB poses a high risk for liver fibrosis, untreated fibrosis is likely to progress to cirrhosis, which imposes a high risk of hepatocellular carcinoma or liver failure [2]. Thus, accurate assessment of liver fibrosis is mandatory to guide therapeutic strategies, helping us prevent and even reverse the process of fibrosis. Liver biopsy has long been regarded as the reference standard for fibrosis diagnosis, but as an invasive means, biopsy can lead to potential complications and

limitations including sampling errors, inter-observer variability and low patient acceptance [3]. Therefore, a reliable non-invasive diagnostic method for liver fibrosis evaluation is in urgent need.

Several noninvasive methods are currently under investigation for the quantification of liver fibrosis. These methods can be divided into two main categories: serum biomarkers and imaging techniques [4]. Combined biochemical markers, such as aspartate aminotransferase-to-platelet ratio index (APRI) and fibrosis index based on the four factors (FIB-4) exhibited promising performance in liver fibrosis evaluation [5,6]. However, the diagnostic utility of these biomarkers is controversial, especially between intermediate fibrosis stages [7,8]. Recent advances in MRI including elastography, diffusion-weighted

* Corresponding author at: Department of Radiology, Zhongshan Hospital, Fudan University, No. 180 Fenglin Road, Xuhui District, Shanghai 200032, China.
E-mail address: ruofansheng@163.com (R.-f. Sheng).

¹ He-qing Wang and Kai-pu Jin contribute the same to the article.

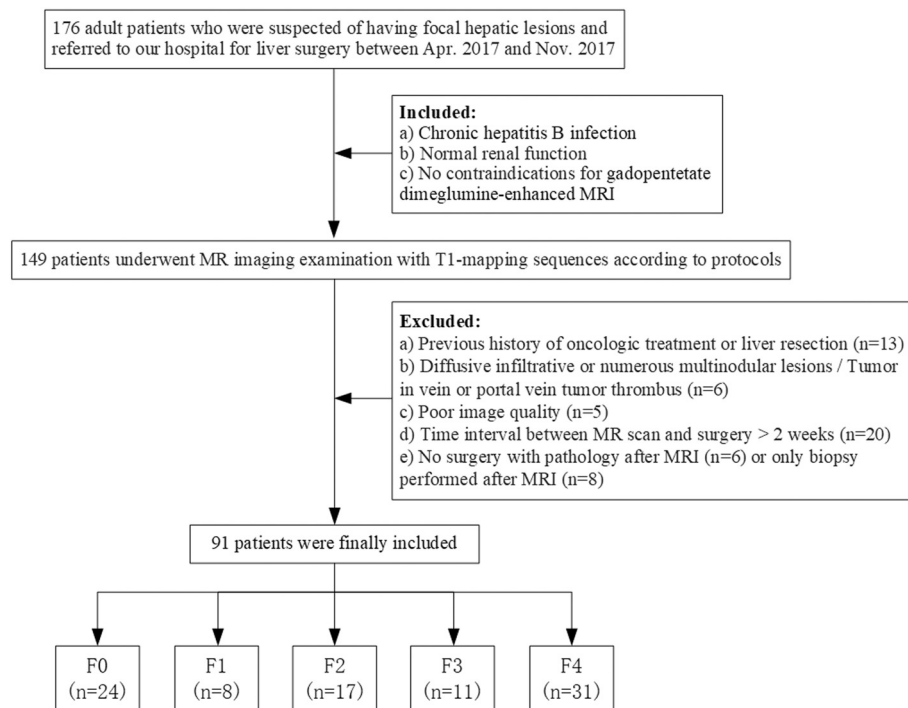


Fig. 1. Flow diagram shows inclusion and exclusion criteria for the study.

imaging, hepatocellular contrast-enhanced MRI, liver surface nodularity, perfusion imaging have made it feasible to evaluate liver fibrosis [9].

Equilibrium imaging is a technique that uses contrast agents widely used in CT and MRI to evaluate the fractional extracellular volume (ECV) that is expanded in fibrosis and other deposition processes [10]. During the equilibrium phase of liver enhancement, the concentration of contrast material is roughly the same in the fluid of the intravascular and extracellular extravascular space, which can be termed the hepatic extracellular space [11]. Previous studies have demonstrated that equilibrium CT imaging may be able to estimate the liver extracellular volume (ECV_{liver}) and have a role in assessment of liver fibrosis [4,10,12]. While the majority application of MR equilibrium imaging for fibrosis assessment limited in the heart [13,14]; few were applied in liver, which were only preliminary studies with limited patient population or no histopathological reference [15,16]. Moreover, the fibrotic patterns may differ among variable etiologies [17]. Therefore, the purpose of this exploratory study was to evaluate the diagnostic value of ECV_{liver} measurement by equilibrium MR in staging liver fibrosis in patients with CHB, and to compare its performance with serum fibrosis indices APRI and FIB-4.

2. Materials and methods

2.1. Patients

Our institutional review board committee on clinical investigation approved the study protocol, and written informed consent was

obtained from each eligible subject before participation. The prospective study enrolled consecutive adult patients who were suspected of having focal hepatic lesions and referred to our hospital for liver surgery between April 2017 and November 2017. Patients with hepatitis B infection (serology test positive for HBV surface antigen) for > 6 months at enrollment, normal renal function (glomerular filtration rate > 90 mL/min/1.73 m²) and no other contraindications for gadopentetate dimeglumine-enhanced MRI underwent MR imaging examination with T1-mapping sequences according to protocols mentioned below in our institute. Exclusion criteria were 1) previous history of oncologic treatment or liver resection; 2) diffusive infiltrative or numerous multinodular lesions that hampered parenchymal evaluation; 3) cases with tumor in vein or portal vein tumor thrombus; 4) difficulty to measure T1 mapping values because of poor image quality (images with poor delineation and significant ghosting and distortion); 5) time interval between MR scan and surgery > 2 weeks; 6) no surgery with pathology or only biopsy performed after MR scanning. Flowchart of the inclusion and exclusion criteria is shown in Fig. 1.

2.2. MR equilibrium imaging

MRI was performed using a 1.5 Tesla scanner (MAGNETOM Aera, Siemens Healthcare, Erlangen, Germany) with phased-array coils. Original images of transverse T1 map was acquired by using 3D gradient echo sequence with volumetric interpolated breath-hold examination (VIBE) sequence with dual flip-angle (FA) method [18], with flip angles of 2° and 12°, which was automatically derived by the Syngo

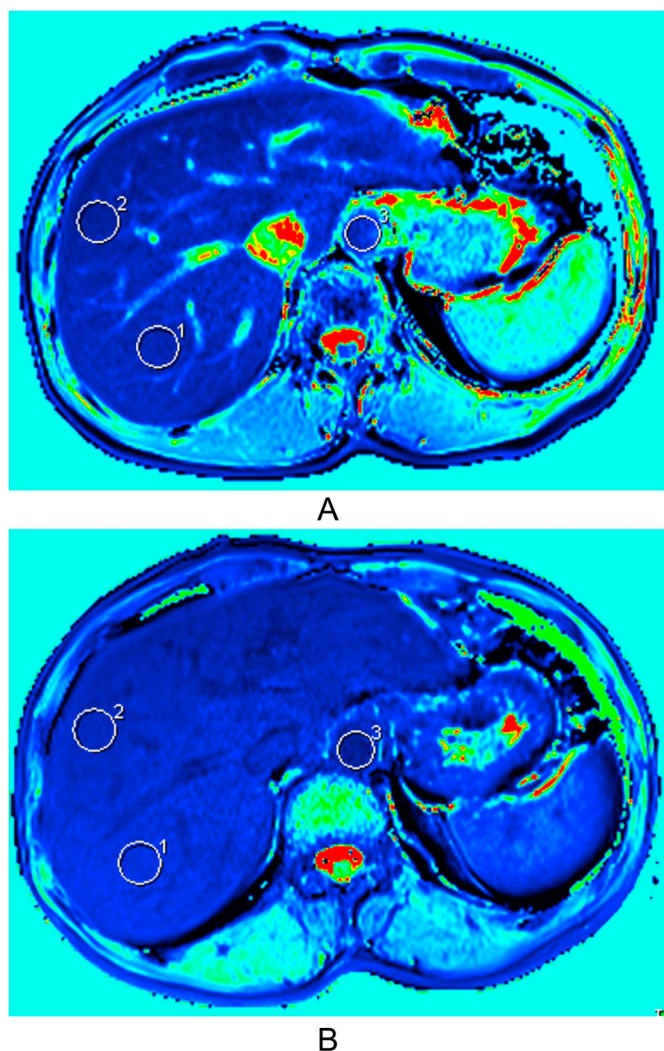


Fig. 2. A 45-year-old male patient with chronic hepatitis B-related liver fibrosis stage 1. Examples of placement of ROIs in the liver parenchyma and aorta on (A) precontrast and (B) equilibrium phase images to measure the T1 relaxation time.

MapIt software (Siemens Healthcare, Erlangen, Germany), based on the given TR = 4.36 ms and estimated target T1 \cong 1000 ms. Parametric T1 maps were inline generated after data acquisition by the MapIt software, using the method described in the reference of Deoni et al. [18]. Detailed parameters were as follows: TE/TR 1.93/4.36 ms, slice thickness 3.5 mm, interslice gap 0.7 mm, FOV 380 \times 285 mm, matrix 162 \times 288. T1 mapping was performed before (pre-contrast) and 15 min after (equilibrium phase) injection of gadopentetate dimeglumine (Magnevist; Bayer Healthcare, Berlin, Germany). Contrast was administered at a dose of 0.1 mmol/kg at a rate of 2 mL/s, followed by a 20 mL saline flush using a power injector (Spectris; Medrad, Pittsburgh,

PA). Equilibrium phase T1 map was conducted 15 min after contrast according to existing literatures [15,16].

2.3. Image analysis

All images were evaluated using a picture archiving and communication system (PACS; Pathspeed, GE Medical Systems Integrated Imaging Solutions, Prospect, IL, USA). Measurements were performed by two abdominal radiologists (with 15 and 4 years of MRI experience) who were blinded to the clinical, laboratory, and histopathologic information; and the interobserver agreement was tested. Measurements from the senior radiologist were used for final calculation and statistics. A total of six regions of interest (ROIs) with a fixed-size of 300 mm² were drawn in the right posterior lobe and right anterior lobe of liver on the central three continuous sections (two ROIs per section), on both pre-contrast and equilibrium phase T1-weighted VIBE images, avoiding large vessels, lesions, artifacts and the border of the liver. The shortest distances between ROIs and large vessels, lesions, as well as liver border were defined as > 1 cm. The ROIs were then copied to T1 map, to measure the T1 relaxation time on a pixel-by-pixel basis. Three further ROIs were drawn at the same slices as large as possible in the lumen of abdominal aorta (mean area, 122.6 mm² and 148.4 mm² for pre-contrast and equilibrium phase images, respectively), with an effort to avoid the aortic wall and any atheromatous plaque. Average values for the ROIs were used. It was tried to place the ROIs at the same axial level on pre- and postcontrast images (Fig. 2).

By using hematocrit measured from the complete blood count and the pre-contrast and equilibrium T1 relaxation time, liver ECV fraction was calculated using the following equation [19]: $ECV_{liver} (\%) = \Delta R1_{liver} / \Delta R1_{aorta} \times (100 - \text{hematocrit})$, where $\Delta R1_{liver} = 1 / T1_{liver \text{ post-contrast}} - 1 / T1_{liver \text{ pre-contrast}}$ and $\Delta R1_{aorta} = 1 / T1_{aorta \text{ post-contrast}} - 1 / T1_{aorta \text{ pre-contrast}}$.

2.4. Pathological analysis

The non-tumorous liver tissues from the resected liver were evaluated for liver fibrosis by a pathologist blinded to the clinical and radiological data (with 21 years of experience in liver pathology). The fibrosis stage (“F” grade) and the necroinflammatory activity (“A” grade) were evaluated by the METAVIR scoring system [20]. The degree of fibrosis was graded using a scale ranging from 0 to 4 (0, no fibrosis; F1, mild fibrosis, portal fibrosis without septa; F2, substantial fibrosis, periportal fibrosis and few septa; F3, advanced fibrosis, septal fibrosis without cirrhosis; F4, cirrhosis). The degree of necroinflammatory activity was graded on a scale of 0 to 3 (A0, none; A1, mild activity; A2, moderate activity; A3, severe activity). We defined stages F0–F1 as no or minimal fibrosis with low likelihood of cirrhosis [21].

2.5. Serum liver fibrosis indices

The concentrations of aspartate transaminase (AST), alanine transaminase (ALT), and platelet (PLT) were obtained from fasting patients on the same day before MR examinations. APRI was calculated using the following formula: $(AST / UL) \times 100 / PLT$, where the upper limit

Table 1
Baseline patient characteristics.

Characteristic	
Sex ^a male/female	68 (74.7)/23 (25.3)
Age (years)	59.0 (51.0, 63.0)
Men	58.0 (51.3, 63.0)
Women	61.0 (46.0, 64.0)
Alanine transaminase (U/L)	24.5 (17.0, 36.0)
Aspartate transaminase (U/L)	23.0 (19.0, 40.0)
Total bilirubin (μmol/L)	11.8 (8.5, 16.5)
Albumin (g/L)	43.0 (41.0, 47.0)
γ-Glutamyl transferase (U/L)	38.0 (24.0, 96.0)
Platelet count ($\times 10^9/L$)	167.0 (117.0, 216.0)
International normalized ratio	1.03 (0.96, 1.07)
APRI	0.414 (0.278, 0.797)
FIB-4	2.00 (1.27, 3.23)
Fibrosis stage ^a	
F0	24 (26.37)
F1	8 (8.79)
F2	17 (18.68)
F3	11 (12.09)
F4	31 (34.07)
Focal liver lesions ^a	
Malignant	79 (86.81)
Benign	12 (13.19)

Unless otherwise stated, data are medians, with interquartile ranges in parentheses.

APRI, aspartate aminotransferase-to-platelet ratio index; FIB-4, fibrosis index based on the four factors.

^a Data are numbers of patients, with percentages in parentheses.

(UL) was considered to be 40 U/L. FIB-4 was calculated as: $\text{Age} \times \text{AST} / (\text{PLT} \times \text{ALT}^{1/2})$. AST and ALT were measured in units per liter, and PLT was measured in $10^9/L$ [22].

2.6. Statistical analysis

Statistical analyses were performed using SPSS software (version 22.0; Chicago, IL, USA) and Medcalc software (version 15.0; Mariakerke, Belgium). Normality of data was tested using the Kolmogorov-Smirnov test, homogeneity of variance was tested using the Levene method. The interobserver agreement of T1 map measurements was assessed by calculating interclass correlation coefficient

Table 2
Statistics of ECV_{liver} , APRI and FIB-4 and the correlation with liver fibrosis.

	F0	F1	F2	F3	F4	<i>r</i>	<i>P</i>
ECV_{liver}	20.40 (17.40–24.85)	26.20 (20.60–30.03)	23.90 (21.05–27.10)	27.90 (24.30–30.80)	33.50 (28.60–37.30)	0.727	< 0.001
APRI	0.281 (0.186–0.363)	0.276 (0.180–0.454)	0.571 (0.293–1.076)	0.404 (0.285–0.901)	0.646 (0.456–0.896)	0.466	< 0.001
FIB-4	1.298 (0.953–2.222)	1.261 (1.133–2.338)	2.051 (1.333–3.057)	2.004 (1.202–3.232)	2.860 (1.657–3.747)	0.440	< 0.001

Data are medians, with interquartile ranges in parentheses.

ECV_{liver} , liver fractional extracellular volume; APRI, aspartate aminotransferase-to-platelet ratio index; FIB-4, fibrosis index based on the four factors.

(< 0.40, poor; 0.40–0.59, fair; 0.60–0.74, good; and 0.75–1.00, excellent). Spearman correlation analysis and stepwise multiple regression analysis were used to measure the strength of the correlation between ECV_{liver} , APRI, FIB-4 and the degree of fibrosis or inflammatory activity. The three indices were compared between different fibrosis subgroups using the one-way ANOVA test or Kruskal–Wallis test. Post hoc multiple comparison of individual mean differences was evaluated by using the least significant difference (LSD) or Dunn post hoc test. Diagnostic performance in evaluating liver fibrosis stages was assessed using receiver operating characteristic (ROC) analysis. The corresponding optimal cutoff values were determined, and areas under the curve (AUCs) with 95% confidence intervals, sensitivity, specificity, positive and negative predictive values for the classification of fibrosis stage F2 or higher, F3 or higher, and F4 were calculated. AUCs were compared using the DeLong method [23]. All tests were two-sided and $P < 0.05$ was considered statistically significant.

3. Results

3.1. Patients

A total of 91 patients (68 men and 23 women; mean age, 59.0 years; range, 28–84 years) were included. The demographic, biochemical, and histological characteristics of all patients are presented in Table 1. The mean interval between MR examination and liver surgery was 6.7 days (range, 1–14 days). Histopathologically, the stages of fibrosis were F0 in 24 (26.37%), F1 in 8 (8.79%), F2 in 17 (18.68%), F3 in 11 (12.09%) and F4 in 31 (34.07%) patients; the grades of necroinflammatory activity were A0 in 23 (25.27%), A1 in 24 (26.37%), A2 in 33 (36.26%) and A3 in 11 (12.09%) patients.

Interobserver agreement showed an excellent interclass correlation coefficient of 0.895 (95% confidence interval: 0.844, 0.929) for ECV_{liver} measurement.

3.2. Relationship between ECV_{liver} , serum fibrosis indices and fibrosis stages

The distributions of ECV_{liver} , APRI, and FIB-4 for different fibrosis stages are shown in Table 2 and Fig. 3. Values were different between groups as a whole ($F/H = 18.44$ to 24.36 , $P \leq 0.001$), although overlaps existed among fibrosis stages. In pairwise comparisons, ECV_{liver} significantly increased between F0 and F1, F0 and F2, F0 and F3, F0 and

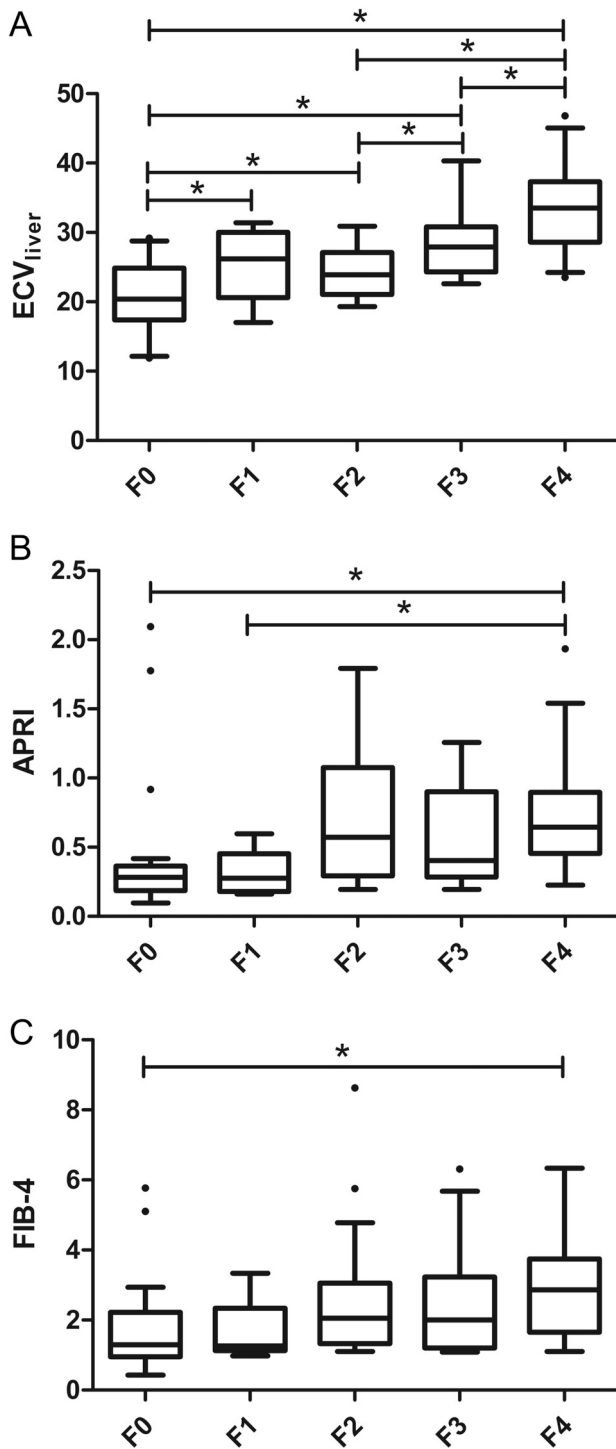


Fig. 3. Box-and-whisker plots show median and ranges for (A) liver extracellular volume (ECV_{liver}), (B) aspartate aminotransferase-to-platelet ratio index (APRI) and (C) fibrosis index based on the four factors (FIB-4) at different stages of liver fibrosis (* represents $P < 0.05$ in pairwise comparisons).

F4, F2 and F3, F2 and F4, F3 and F4; APRI significantly increased between F0 and F4, F1 and F4; and FIB-4 significantly increased between F0 and F4 ($P < 0.05$).

ECV_{liver} had the strongest correlation with fibrosis stage ($r = 0.727$, $P < 0.001$), while APRI and FIB-4 had weak correlations ($r = 0.466$ and 0.440 , $P < 0.001$). Among the three noninvasive methods, multivariate analysis showed that only ECV_{liver} was independently correlated with fibrosis stage ($P < 0.001$). Significant but weaker correlation existed between ECV_{liver} and inflammatory activity ($r = 0.503$, $P < 0.001$). Although both fibrosis stage and inflammatory activity were significantly correlated with ECV_{liver}, the fibrosis stage was the only independent factor ($P < 0.001$).

3.3. Diagnostic performance of ECV_{liver} and serum fibrosis indices in fibrosis staging

ROC curves and the corresponding diagnostic performance of ECV_{liver}, APRI, and FIB-4 for prediction of various fibrosis stages are shown in Table 3 and Fig. 4. The AUC values of ECV_{liver}, APRI, and FIB-4 were 0.824, 0.782, and 0.751 for fibrosis stage 2 or higher; 0.898, 0.710 and 0.708 for stage 3 or higher; and 0.907, 0.735, and 0.729 for stage 4, respectively. In general, AUCs of ECV_{liver} were larger than both APRI and FIB-4 in fibrosis staging, with significant differences in the diagnosis of advanced fibrosis ($\geq F3$) and cirrhosis (F4) ($P = 0.0024$ to 0.0049); although no significant differences existed for the diagnosis of substantial fibrosis ($\geq F2$) in pairwise comparisons ($P = 0.582$ and 0.296).

4. Discussion

Our study concluded that a simple calculation of ECV_{liver} by equilibrium MR had excellent interobserver agreement, stronger correlation with fibrosis, and better diagnostic performance in fibrosis staging, especially for identification of advanced fibrosis and cirrhosis, in comparison with APRI and FIB-4; providing a promising imaging biomarker in predicting the severity of liver fibrosis for CHB patients.

The present study showed that ECV_{liver} had a significant correlation with liver fibrosis stage, consistent with previous studies: Wells et al. [16] pointed out that MR hepatic fractional extracellular space correlated modestly with liver stiffness measured at MRE, but they used signal intensity instead of T1 values without histopathological reference; Luetkens et al. [15] conducted a preliminary study in 10 patients recently and showed a correlation between ECV fraction and percentage of sirius red staining, but the results were limited due to the restricted patient population and no exact fibrosis staging. The essential histopathologic feature of hepatic fibrosis is the expansion of the extracellular matrix secondary to the deposition of collagen and matrix proteins [4,11,12]. Therefore, ECV in fibrotic regions would be higher than normal liver parenchyma, and would increase with the progression of liver fibrosis.

Edema from inflammation may expand ECV_{liver} and confound fibrosis measurement [10]. Our study indicated that fibrosis stage was the only factor independently predicted by ECV_{liver}. Thus, we considered ECV_{liver} a reliable tool in assessing liver fibrosis.

In our study, ECV_{liver} appeared to be somewhat superior to APRI and FIB-4 in fibrosis evaluation, especially in the diagnosis of

Table 3
Diagnostic performance of ECV_{liver}, APRI and FIB-4 for evaluating different fibrosis stages.

	AUC (95% CI)	Cutoff	Sen (%)	Spe (%)	PPV (%)	NPV (%)
ECV_{liver}						
≥ F2	0.824 (0.730, 0.896)	> 26.6	67.80	81.25	87.0	57.8
≥ F3	0.898 (0.817, 0.952)	> 27.6	78.57	87.76	84.6	82.7
F4	0.907 (0.828, 0.958)	> 27.6	87.10	80.00	69.2	92.3
APRI						
≥ F2	0.782 (0.683, 0.862)	> 0.310	81.36	67.74	82.8	65.6
≥ F3	0.710 (0.605, 0.801)	> 0.310	88.10	56.25	63.8	84.4
F4	0.735 (0.632, 0.823)	> 0.429	80.65	69.49	57.9	85.7
FIB-4						
≥ F2	0.751 (0.649, 0.836)	> 1.558	72.88	70.97	82.7	57.9
≥ F3	0.708 (0.603, 0.799)	> 1.604	73.81	62.50	63.3	73.2
F4	0.729 (0.625, 0.818)	> 1.529	87.10	50.85	48.2	88.2

ECV_{liver}, liver fractional extracellular volume; APRI, aspartate amino-transferase-to-platelet ratio index; FIB-4, fibrosis index based on the four factors; AUC, area under the curve; CI, confidence interval; Sen, sensitivity; Spe, specificity; PPV, positive predictive value; NPV, negative predictive value.

advanced fibrosis and cirrhosis. The risk of complications as a result of fibrosis including cirrhosis and HCC starts to increase in F3 fibrosis [24,25]; and cirrhosis is most strongly associated with liver-related morbidity and mortality [21]; which are therefore both clinically important stage to identify noninvasively. Additionally, serum panels cannot reliably quantify regional distribution of hepatic fibrosis [4]; while MR ECV_{liver} has the potential to sample the entire liver volume and the ability to detect regional variation of fibrosis, as multiple regions of interest could easily be used [16]. We recommended MR ECV_{liver} a better tool in evaluating liver fibrosis and a potential method to demonstrate the heterogeneity. Meanwhile, although AUCs of ECV_{liver} were also larger than both APRI and FIB-4 in identification of substantial fibrosis, the diagnostic performance was barely satisfactory with no statistical significance. The key factors in initial fibrogenesis are the activation and proliferation of hepatic stellate cells (HSCs), and a large number of HSCs has been activated before extensive deposition of extracellular matrix [26,27]. Thus, ECV_{liver} quantification may not reflect the very early stage of liver fibrosis. Our limited patient population of early fibrosis stage may also influence the statistical power.

This study had certain limitations. First, the levels of liver fibrosis were not uniformly balanced with a large percentage of cirrhosis; this is because a large percentage of included patients had hepatocellular carcinoma with accompanying cirrhosis liver background. Additionally, the sample size of fibrosis stage 1 was relatively small, we combined stages F0 and F1 as no or minimal fibrosis. Further study with larger and more uniform sample size is necessary. Second, we focused on the comparison analyses with serum fibrosis indices in this study, and did not compare ECV_{liver} with other imaging methods used in liver fibrosis assessment including ultrasound and MR elastography, which should be further investigated in future work.

In conclusion, ECV_{liver} measurement by equilibrium MR provides a promising noninvasive tool in predicting the severity of liver fibrosis for CHB patients, especially in the identification of advanced fibrosis and cirrhosis, superior to the serum fibrosis indices of APRI and FIB-4. It is a scanning protocol without additional equipment and is based on simple calculations, we consider that MR ECV_{liver} may be implemented to routine clinical liver MR examinations.

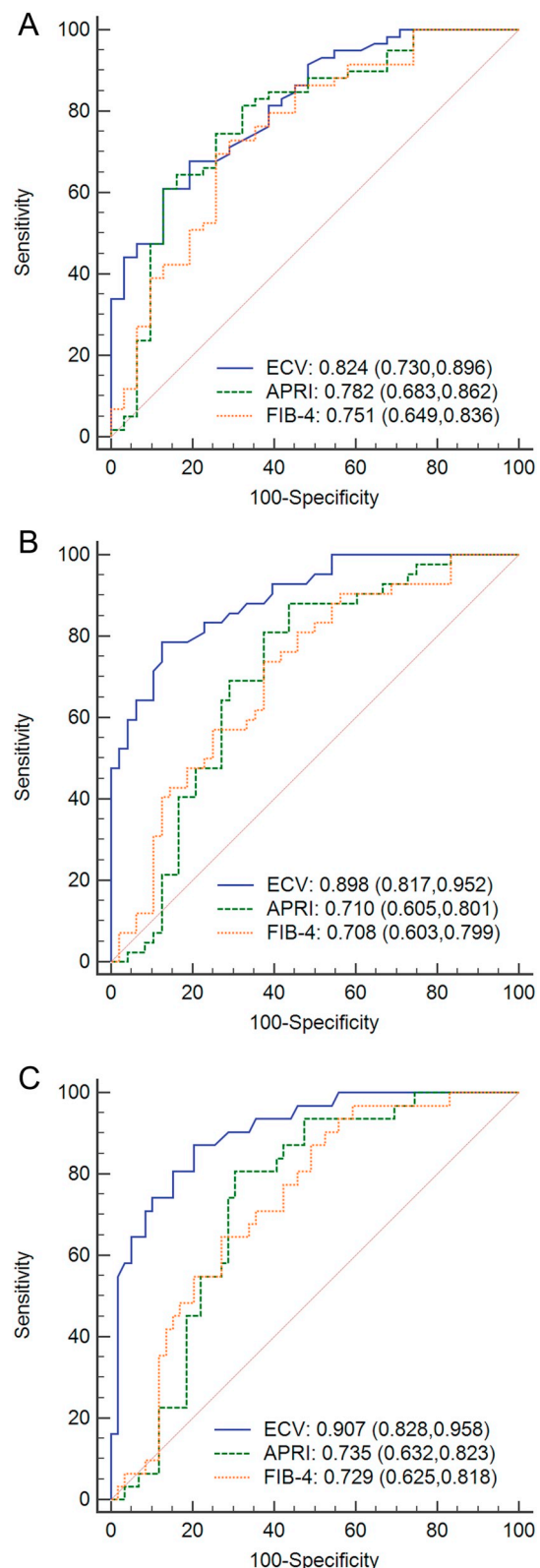


Fig. 4. Receiver operating characteristic curves for the identification of liver fibrosis stages (A) F ≥ 2, (B) F ≥ 3, and (C) F4 using liver extracellular volume (ECV_{liver}), aspartate aminotransferase-to-platelet ratio index (APRI), and fibrosis index based on the four factors (FIB-4). Numbers are areas under the curve with 95% confidence intervals in parentheses.

Declarations of interest

None.

Acknowledgements

None.

Funding

This study was funded by the National Natural Science Foundation for Young Scientists of China (grant number 81601488), the Shanghai Sailing Program (grant number 16YF1410600), and the National Natural Science Foundation of China (grant number 81571661).

References

- [1] Lok AS, McMahon BJ, Brown Jr. RS, Wong JB, Ahmed AT, Farah W, et al. Antiviral therapy for chronic hepatitis B viral infection in adults: a systematic review and meta-analysis. *Hepatology* 2016;63:284–306. <https://doi.org/10.1002/hep.28280>.
- [2] Polasek M, Fuchs BC, Uppal R, Schuehle DT, Alford JK, Loving GS, et al. Molecular MR imaging of liver fibrosis: a feasibility study using rat and mouse models. *J Hepatol* 2012;57:549–55. <https://doi.org/10.1016/j.jhep.2012.04.035>.
- [3] Yoon JH, Lee JM, Baek JH, Shin C-i, Kiefer B, Han JK, et al. Evaluation of hepatic fibrosis using intravoxel incoherent motion in diffusion-weighted liver MRI. *J Comput Assist Tomogr* 2014;38:110–6. <https://doi.org/10.1097/RCT.0b013e3182a589be>.
- [4] Varenika V, Fu Y, Maher JJ, Gao D, Kakar S, Cabarrus MC, et al. Hepatic fibrosis: evaluation with semiquantitative contrast-enhanced CT. *Radiology* 2013;266:151–8. <https://doi.org/10.1148/radiol.12112452>.
- [5] Xiao GQ, Yang JY, Yan LA. Comparison of diagnostic accuracy of aspartate aminotransferase to platelet ratio index and fibrosis-4 index for detecting liver fibrosis in adult patients with chronic hepatitis B virus infection: a systemic review and meta-analysis. *Hepatology* 2015;61:292–302. <https://doi.org/10.1002/hep.27382>.
- [6] Teshale E, Lu M, Rupp LB, Holmberg SD, Moorman AC, Spradling P, et al. APRI and FIB-4 are good predictors of the stage of liver fibrosis in chronic hepatitis B: the Chronic Hepatitis Cohort Study (CHecs). *J Viral Hepat* 2014;21:917–20. <https://doi.org/10.1111/jvh.12279>.
- [7] Kim WR, Berge T, Asselah T, Flisiak R, Fung S, Gordon SC, et al. Evaluation of APRI and FIB-4 scoring systems for non-invasive assessment of hepatic fibrosis in chronic hepatitis B patients. *J Hepatol* 2016;64:773–80. <https://doi.org/10.1016/j.jhep.2015.11.012>.
- [8] Ucar F, Sezer S, Giris Z, Ozturk G, Albayrak A, Basar O, et al. APRI, the FIB-4 score, and Forn's index have noninvasive diagnostic value for liver fibrosis in patients with chronic hepatitis B. *Eur J Gastroenterol Hepatol* 2013;25:1076–81. <https://doi.org/10.1097/MEG.0b013e31832835fd699>.
- [9] Mathew RP, Venkatesh SK. Imaging of hepatic fibrosis. *Curr Gastroenterol Rep* 2018;20(45). <https://doi.org/10.1007/s11894-018-0652-7>.
- [10] Bandula S, Punwani S, Rosenberg WM, Jalan R, Hall AR, Dhillon A, et al. Equilibrium contrast-enhanced CT imaging to evaluate hepatic fibrosis: initial validation by comparison with histopathologic analysis. *Radiology* 2015;275:136–43. <https://doi.org/10.1148/radiol.14141435>.
- [11] Zissen MH, Wang ZJ, Yee J, Aslam R, Monto A, Yeh BM. Contrast-enhanced CT quantification of the hepatic fractional extracellular space: correlation with diffuse liver disease severity. *AJR Am J Roentgenol* 2013;201:1204–10. <https://doi.org/10.2214/ajr.12.10039>.
- [12] Guo SL, Su LN, Zhai YN, Chirume WM, Lei JQ, Zhang H, et al. The clinical value of hepatic extracellular volume fraction using routine multiphase contrast-enhanced liver CT for staging liver fibrosis. *Clin Radiol* 2017;72:242–6. <https://doi.org/10.1016/j.crad.2016.10.003>.
- [13] Everett RJ, Stirrat CG, Semple SIR, Newby DE, Dweck MR, Mirsadraee S. Assessment of myocardial fibrosis with T1 mapping MRI. *Clin Radiol* 2016;71:768–78. <https://doi.org/10.1016/j.crad.2016.02.013>.
- [14] Schelbert EB, Messroghli DR. State of the art: clinical applications of cardiac T1 mapping. *Radiology* 2016;278:658–76. <https://doi.org/10.1148/radiol.2016141802>.
- [15] Luetkens JA, Klein S, Traeber F, Schmeel FC, Sprinkart AM, Kuetting DLR, et al. Quantitative liver MRI including extracellular volume fraction for non-invasive quantification of liver fibrosis: a prospective proof-of-concept study. *Gut* 2018;67:593–4. <https://doi.org/10.1136/gutjnl-2017-314561>.
- [16] Wells ML, Moynagh MR, Carter RE, Childs RA, Leitch CE, Fletcher JG, et al. Correlation of hepatic fractional extracellular space using gadolinium enhanced MRI with liver stiffness using magnetic resonance elastography. *Abdom Radiol (NY)* 2017;42:191–8. <https://doi.org/10.1007/s00261-016-0867-8>.
- [17] Pinzani M, Rombouts K, Colagrande S. Fibrosis in chronic liver diseases: diagnosis and management. *J Hepatol* 2005;42(Suppl):S22–36. <https://doi.org/10.1016/j.jhep.2004.12.008>.
- [18] Deoni SC, Rutt BK, Peters TM. Rapid combined T1 and T2 mapping using gradient recalled acquisition in the steady state. *Magn Reson Med* 2003;49:515–26. <https://doi.org/10.1002/mrm.10407>.
- [19] Bandula S, Banypersad SM, Sado D, Flett AS, Punwani S, Taylor SA, et al. Measurement of tissue interstitial volume in healthy patients and those with amyloidosis with equilibrium contrast-enhanced MR imaging. *Radiology* 2013;268:858–64. <https://doi.org/10.1148/radiol.13121889/-/DC1>.
- [20] Goodman ZD. Grading and staging systems for inflammation and fibrosis in chronic liver diseases. *J Hepatol* 2007;47:598–607. <https://doi.org/10.1016/j.jhep.2007.07.006>.
- [21] Barr RG, Ferraioli G, Palmeri ML, Goodman ZD, Garcia-Tsao G, Rubin J, et al. Elastography assessment of liver fibrosis: Society of Radiologists in Ultrasound consensus conference statement. *Radiology* 2015;276:845–61. <https://doi.org/10.1148/radiol.2015150619>.
- [22] Zhuang Y, Ding H, Zhang Y, Sun HC, Xu C, Wang WP. Two-dimensional shear-wave elastography performance in the noninvasive evaluation of liver fibrosis in patients with chronic hepatitis B: comparison with serum fibrosis indexes. *Radiology* 2017;283:872–81. <https://doi.org/10.1148/radiol.2016160131>.
- [23] Delong ER, Delong DM, Clarkepearson DL. Comparing the areas under two or more correlated receiver operating characteristic curves: a nonparametric approach. *Biometrics* 1988;44:837–45. <https://doi.org/10.2307/2531595>.
- [24] Ding Y, Rao SX, Zhu T, Chen CZ, Li RC, Zeng MS. Liver fibrosis staging using T1 mapping on gadoteric acid-enhanced MRI compared with DW imaging. *Clin Radiol* 2015;70:1096–103. <https://doi.org/10.1016/j.crad.2015.04.014>.
- [25] Ikeda K, Saitoh S, Suzuki Y, Kobayashi M, Tsubota A, Koida I, et al. Disease progression and hepatocellular carcinogenesis in patients with chronic viral hepatitis: a prospective observation of 2215 patients. *J Hepatol* 1998;28:930–8.
- [26] Friedman SL. Liver fibrosis — from bench to bedside. *J Hepatol* 2003;38(Suppl. 1):S38–53.
- [27] Moreira RK. Hepatic stellate cells and liver fibrosis. *Arch Pathol Lab Med* 2007;131:1728–34. [https://doi.org/10.1043/1543-2165\(2007\)131\[1728:hscalf\]2.0.co;2](https://doi.org/10.1043/1543-2165(2007)131[1728:hscalf]2.0.co;2).